NTNU – Trondheim
Norwegian University of
Science and Technology

Calculation of Transition Moments Using the Extended Coupled Cluster Model ECC2

Kristin Marie Skjelbred

Chemical Engineering and Biotechnology
Submission date: June 2014
Supervisor: Henrik Koch, IKJ

Norwegian University of Science and Technology
Department of Chemistry

Abstract

As a part of the ongoing development of the multi level coupled cluster (MLCC) model ECC2, the work presented here is focused on obtaining transition moments associated with certain excitation energies. The ECC2 model divides the system into two subsystems where different levels of theory are used. The idea behind the method is to use a high level of theory on a small part of the system, the active space, and a lower level on the bigger part, the inactive space. Specifically the coupled cluster singles and doubles (CCSD) is used as the higher level, while the approximate model CC2 is used as the lower level. This allows for retention of computational accuracy while reducing the complexity and consequently the cost of the calculations, assuming the active space has been chosen correctly.

An important part of MLCC theory is the partitioning of the system and how orbitals are described. Here Cholesky decomposition has been chosen, both because it reduces computational complexity and because it lets the user use his chemical expertise. The former is a consequence of when the positive semidefinite density matrix is decomposed into a lower triangular matrix and its tranpose, and then used to generate localized orbitals. The orbitals are assigned to atomic centers, and since it is up to the user to choose which orbitals are part of the active space, use of chemical intuition is key. Transition moments are a local property and limiting the active space to the orbitals taking part in the corresponding excitation leads to a great reduction in scaling.

A pilot version of the model is tested and compared to CCSD and CC2. The outcome of the testing suggests that the current version of the code still contains bugs and needs to be modified, but also show that parts of the model have successfully been implemented. The accuracy of the results presented here are not discussed, as they have proven to be different than expected and suggest further testing and debugging of the code, before the ECC2 transition moments are published.

Sammendrag

Som en del av den pågående utviklingen av *multi level coupled cluster* (MLCC) modellen ECC2 er arbeidet som er presentert her, fokusert på å beregne overgangsmomentene som er assosiert med bestemte eksitasjonsenergier. ECC2-modellen deler opp systemet i to undersystemer hvor ulike teorinivåer er brukt. Ideen bak metoden er å bruke et høyere nivå på en liten del av systemet, det aktive rommet, og et lavere nivå på den største delen, det inaktive rommet. Spesifikt er det *coupled cluster singles and doubles* (CCSD) som brukes for det aktive rommet, mens den mindre nøyaktige modellen CC2 brukes for det inaktive rommet. Dette gjør det mulig å opprettholde beregningsnøyaktigheten, samtidig som man får redusert kompleksiteten og dermed prisen på beregningene. Dette forutsetter riktig valg av aktivt rom.

En viktig del av MLCC-teori er inndelingen av systemet og hvordan orbitalene er beskrevet. Her er Cholesky-dekomponering brukt, både fordi det reduserer kompleksiteten av beregningene, og fordi det lar brukeren bruke sin kjemiskekunnskap. Det første er en konsekvens av at den positive semidefinitte tetthetsmatrisen er dekomponert i en nedre triangulær matrise og dens transponerte, for så å brukes til genereringen av lokaliserte orbitaler. Orbitalene er tilskrevet atomiske sentra, og fordi det er opp til brukeren å velge hvilke orbitaler som skal være en del av det aktive rommet, er kjemisk intuisjon essensielt. Overgangsmomenter er en lokal egenskap, og ved å begrense det aktive rommet til orbitalene som tar del i den tilsvarende eksitasjonen, vil man få en kraftig redusert skalering.

En pilotversjon av modellen er testet og sammenlignet med CCSD og CC2. Utfallet av testingen viser at den nåværende versjonen av koden fremdeles inneholder programvarefeil og derfor må modifiseres, men de tyder også på at deler av modellens implementering har vært vellykket. Nøyaktigheten til resultatene som er presentert her er ikke diskutert i og med at de viser seg å avvike fra det som er forventet og antyder at koden bør utvikles og testes videre før ECC2-overgangsmomentene kan publiseres.

Preface

This thesis concludes my five year education in Chemical Engineering and Biotechnology at the Norwegian University of Science and Technology. Early on in the program my curiosity for the underlying physical principles in chemistry was awakened, and I chose to focus the final years of my M. Tech. Degree in the field of Applied Theoretical Chemistry.

This project has allowed me to develop myself as a theoretical and computational chemist, but I would not have been able to accomplish what I have without the help and guidance of my supervisor Professor Henrik Koch and his infinitely patient and helpful Ph.D. candidate Rolf H. Myhre. Thank you both so much. The opurtunity of working on an ongoing research project has been challenging, but it has also encouraged me to pursue an academic career.

Finally I want to thank my parents, family and friends that have all supported me through these five difficult, yet rewarding years. A special thanks to my mother and John Naviaux for proofreading.

Kristin Marie Skjelbred
Trondheim, June 6^{th} 2014

Contents

1 Introduction

1.1 Motivation

The evolution of supercomputers has accelerated the potential of computatonal chermistry and let theoretical chemists develop and test ideas that were infeasible only decades ago [1, 2]. It is now possible to use quantum mechanical (QM) methods on small systems to obtain highly accurate results. The most rigorous theoretical models are even more accurate than present experimental methods [3]. For larger systems, however, the methods soon become too computationally costly due to scaling up of the resource heavy calculations. It is therefore more common to use lower level methods in QM or other methods, such as molecular mechanics (MM) or density functional theory (DFT) for large systems. MM cannot give answers to all the questions QM can, but it can be combined with a QM method [4, 5]. DFT, on the other hand, is less reliable than QM due to the uncertainty rising from the use of the density functionals used to describe the electron density [6, 7, 8].

Another possibility is to use a multilevel QM method where a higher level method is used only on the part of the system that is most interesting, for instance the orbitals taking part in an electron excitation. A lower level method is then used on the remaining part of the system. Using a multilevel method makes it possible to achieve results comparable to using the higher level method on the whole system [9]. This is not a black box scenario, and a thorough understanding of the chemistry involved is therefore necessary. The work presented here is based on coupled cluster (CC) theory and is a continuation of the developement of the multilevel CC method, extended CC2 (ECC2). In this model the biggest part of the system is treated with the approximate (CC2) model and a small part of the system is treated with the higher level coupled cluster singles and doubles (CCSD) model. As shown by Myhre et al.[9], the ECC2 model gives significantly better results than CC2, while retaining the N^5 scaling compared to the N^6 scaling of the CCSD model, where N is the number of orbitals. In the hierarchy of CC models, the CC2 model enters between coupled-cluster singles (CCS) and CCSD [10] and

can be compared to a fusion of second-order Møller-Plesset theory (MP2) and the second-order polarization propagator approximation (SOPPA). Compared to configuration interaction (CI) models, CC with the same parameter space recovers more of the excitation energy for short bond lengths [11]. While the CI approach will recover more of the excitation energy as the bond lengths increases, the CC performance will degrade. Olsen et. al (1996) found that at the equilibrium bond length, the CCSD recovers more of the correlation energy than the configuration-interaction singles, doubles and triples (CISDT). One feature of the ECC2 model that differs from a single level method is that it lets the user apply his chemical intuition when assigning what part of the system is to be treated with which level of theory, i.e. this is not a black box model. The partitioning of the system is something that must be taken into careful consideration as this will affect the computational cost as well as the outcome. Myhre et al. used Cholesky decomposition [12] to generate orbitals that were located on atoms instead of using molecular orbitals. Cholesky decomposition has proven to reduce scaling [13, 14, 15], so by carefully assigning active spaces, sublinearly scaling can be achieved and so the ECC2 model should be able to compete with DFT.

The ECC2 model will make it possible to achieve more accurate results at a lower cost than today's established methods, and can be used on more complex systems, such as biological ones, to broaden our understanding and knowledge about such systems. The method is applicable to medical research, the development of drugs, and many of the challenges caused by the increasing complexity of the oil and gas industry. The model has previously been tested on excitation energies [9] and the work presented here is focused on transition moments of the excitations. From the transition moment one can determine whether a transition is allowed or not [3], and they are therefore important when the ECC2 model is to be implemented and used for scientific purposes. The square of the transition moment is proportional to the intensity of the transition and related to the probability of it occuring [16, 17]. The transition moment is thus used to identify the spectrum of the molecules [18]. This is important when comparing the computational method to experimental data, and therefore a motivation for the development of less costly methods that retain accuracy to be used on more complex systems. Because excitation energies

and transition moments are local properties, a multilevel method is expected to be a good approximation [19]. The derivation is based on the quasienergy response method, and both the excitation energy and the transition moment are calculated from the linear response function [20].

1.2 Outline of the Thesis

Background theory is first presented followed by the derivation of the necessary equations. An implementation plan for the DALTON software package is then described. The current version of the code is then tested and discussed in comparison to CC2 and CCSD results. After a conclusion of the work done so far, a description of the future work is suggested.

2 Theory

After an introduction to coupled cluster theory, Cholesky decomposition and response theory, the ECC2 transition moment is derived. The background is explained in Sec. 2.1 - 2.4 and the derivation is shown in Sec. 2.5. The Hamiltonian is constructed using the Born-Oppenheimer approximation and is represented by two creation and annihilation operators, $a^\dagger$ and a, from second quantization. [21]

$$H = \sum_{pq} h_{pq} a_p^\dagger a_q + \frac{1}{2} \sum_{pqrs} (pq|rs)\, a_p^\dagger a_q^\dagger a_r a_s + h_{nuc} \tag{2.1}$$

In Eq. (2.1) the contributions are given by

$$h_{pq} = \int \phi_p^*(x) \left(-\frac{1}{2}\nabla^2 - \sum_I \frac{Z_I}{r_I} \right) \phi_q(x) dx \tag{2.2}$$

$$(pq|rs) = \int\int \frac{\phi_p^*(x_1)\phi_r^*(x_2)\phi_q(x_1)\phi_s(x_2)}{r_{12}} dx_1 dx_2 \tag{2.3}$$

$$h_{nuc} = \frac{1}{2} \sum_{I \neq J} \frac{Z_I Z_J}{R_{IJ}} \tag{2.4}$$

where Z_I is the nuclear charge of nucleus I, r_I the electron-nuclear separations, r_{12} the electron-electron separation, R_{IJ} the internuclear separations, and ϕ refers to spin-orbitals. Eq. (2.2) and (2.3) can be interpreted as "amplitudes" of single and double excitations respectively while Eq. (2.4) represents the nuclear repulsion energy.[3]

2.1 Coupled Cluster Theory

The coupled cluster (CC) method is best viewed as a correction to the Hartree-Fock (HF) description, as it cannot be applied to systems with a nearly degenerate electronic configuration. The CC method should thus be applied to systems that are dominated by a single electronic configuration, and the method has indeed proven to be a successful approach to describing electron correlation for such systems [22, 23, 24, 25]. The method can be described as a product of creation and

anihilation operators. A pair cluster is used as an example in Eq. (2.5).

$$\tau_{IJ}^{AB} = a_A^\dagger a_I a_B^\dagger a_J \tag{2.5}$$

τ_{IJ}^{AB} is an operator that describes the correlated excitation of two electrons initially occupying the spin oribitals I and J, to two spin orbitals A and B, initially unoccupied. For the general excitation τ_μ, the CC wave function may be expressed as a product of excitation operators and their amplitudes, t_μ, using the the fact that only one electron can occpy each spin orbital, i.e.

$$\tau_{IJ}^{AB}\tau_{IJ}^{CD} = 0 \tag{2.6}$$

Excitation μ is then given by Eq. (2.7) while the CC wave function takes the form shown in Eq. (2.8).

$$|\mu\rangle = \tau_\mu |HF\rangle \tag{2.7}$$

$$|CC\rangle = \left[\prod_\mu (1 + t_\mu \tau_\mu)\right] |HF\rangle \tag{2.8}$$

For practical use, it is more common to express the CC wave function using the exponential ansatz.

$$|CC\rangle = \exp\left(X(t)\right) |HF\rangle \tag{2.9}$$

Where $X(t)$ is the time-dependent cluster operator defined in Eq. (2.11) and we have used that

$$1 + t_\mu \tau_\mu = \exp(t_\mu \tau_\mu) \tag{2.10}$$

$$X\left(t\right) = \sum_\mu t_\mu\left(t\right) \tau_\mu \tag{2.11}$$

The exponential ansatz can be used because the excitation operators commute [3]. This can be proven using creation and annihilation operators and their anticommutation relations.

$$[\tau_\mu, \tau_\nu] = 0 \tag{2.12}$$

2.2 Multi-Level Coupled-Cluster Theory

There are different levels of CC theory, and the simplest one is where all single excitations (CCS) within the given basis set are included, and corresponds to Hartree-Fock theory. While the single excitations represent a relaxation of the spin orbitals, the double excitations contribute significantly to the description of the electronic system [3]. This can be explained by the fact that only two electrons (with opposite spin) can occupy the same spatial orbital. The closer two electrons are to each other, the more significant their interaction will be. Excitations of higher levels, such as double, triple and quadruple can also be taken into account. The cluster operator is then truncated depending on which level of theory is to be implemented. As the comptational cost increases with the level of theory, this is something that needs to be taken into consideration even though highly accurate models such as CCSDTQ [26] and even up to CCSDTQ567 [27] have been implemented. For large systems, however, scaling soon becomes a problem. Even though coupled-cluster singles and doubles (CCSD) can be used for systems containing more than 25 atoms, biological systems often contain hundreds of atoms, making the quantum chemical calculations too expensive. This is why approximate methods, such as CC2 have been developed. The CC2 method lies between CCS and CCSD in the CC hierachy and includes all single excitations, but double excitations only up to first order [10]. CC2 computations give results that are closer to CCS than CCSD. Another popular approximate model is the CCSD(T), where the triple excitations are treated non-iteratively [28, 29]. By dividing the system and treating the most important part with CCSD and the remaining part with CC2, Myhre et al. were able to achieve results closer to CCSD accuracy. This multi-level CC model is called extended CC2 (ECC2) and the theory behind this specific model is explained more thoroughly in the following sections.

2.2.1 Cholesky Decomposition

In general multi-level coupled-cluster (MLCC) theory, the orbital space can be divided into two or more subsystems where each subsystem is treated with different levels of theory, and excitations between levels can be assigned to either the higher or the lower level. However, it is important to take the partitioning of the system into careful consideration. A simple way is to assign the lowest energy unoccupied molecular orbital and the highest energy occupied molecular orbital to the active space and treat the rest of the system as the inactive space. However, this might give rise to problems as changing the geometry of a molecule will affect the energy of the orbitals. This can be avoided using Cholesky decomposition to generate localized orbitals that resemble the classic Lewis structures [12, 30]. These orbitals are generated from the one-electron Hartree-Fock (HF) density matrix, $\boldsymbol{D}$ given by

$$D_{\alpha\beta} = \sum_{i}^{occ} C_{\alpha i} C_{\beta i} \tag{2.13}$$

where $C_{\alpha i}$ is the coeffcient expanding the occupied molecular orbital (MO) i from the atomic orbital α. Similarly for the virtual orbitals, the pseudodensity matrix $\boldsymbol{D}^V$ consists of the elements

$$D^V_{\alpha\beta} = \sum_{a}^{virt} C_{\alpha a} C_{\beta a} \tag{2.14}$$

Both Eq. (2.13) and (2.14) give positive semidefinite matrices and their rank is the number of occupied and virtual orbitals respectively. These matrices are then decomposed into a lower triangular matrix $\boldsymbol{L}$ and its transpose

$$\boldsymbol{D} = \boldsymbol{L}\boldsymbol{L}^T \tag{2.15}$$

The fact that both $\boldsymbol{D}$ and $\boldsymbol{D}^V$ are positive semidefinite causes the Cholesky decomposition to not be unique, and therefore the pivoting scheme gives rise to different decompositions. This is used to generate localized active spaces. An advantage of

Cholesky decomposition compared to alternatives such as linear scaling methods using multipole expansion of the two-electron Coulomb interaction [31], is that it does not deteriorate as the size of the basis set increases [32]. Atoms that are of higher interest than others are considered active and the decomposition is only done for the active space. This results in MOs that are assigned to an atomic center. The pivoting is done for both the occupied and virtual orbitals and the number of spaces depends on how many levels of theory it is appropriate to use. In the ECC2 model only two levels are used, but one could also choose to add a third level of CCS, or even a fourth level where no excitations are considered, i.e. HF. The following figures show an example of decanal with three levels of theory, and are a courtesy of Alfredo Sánchez de Merás k[33].

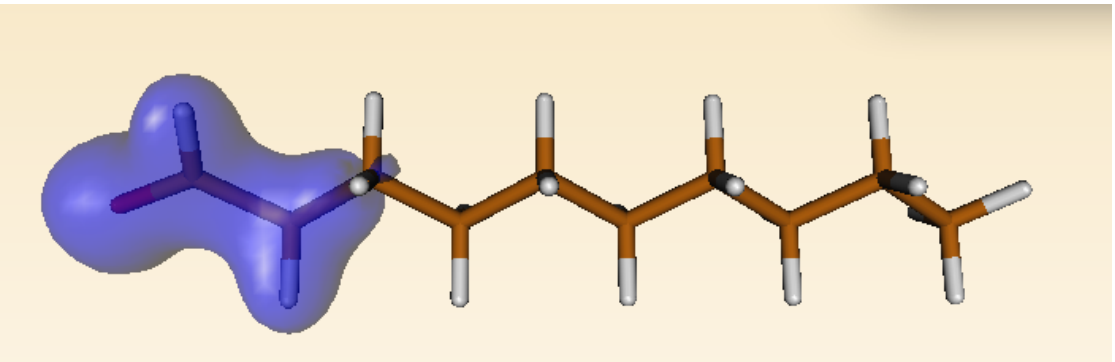

Figure 1: CCSD space of decanal.

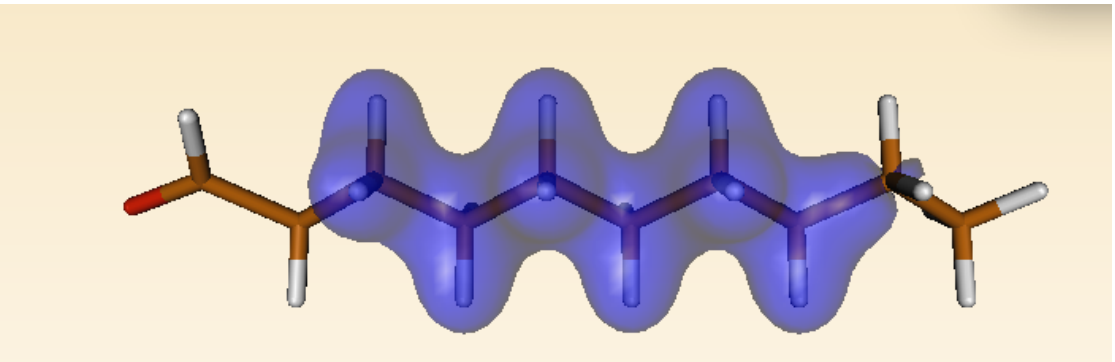

Figure 2: CC2 space of decanal.

Figure 1 shows which atoms are part of the active space, treated with CCSD. This is only a small part of the molecule, and is of most significance to the result. The

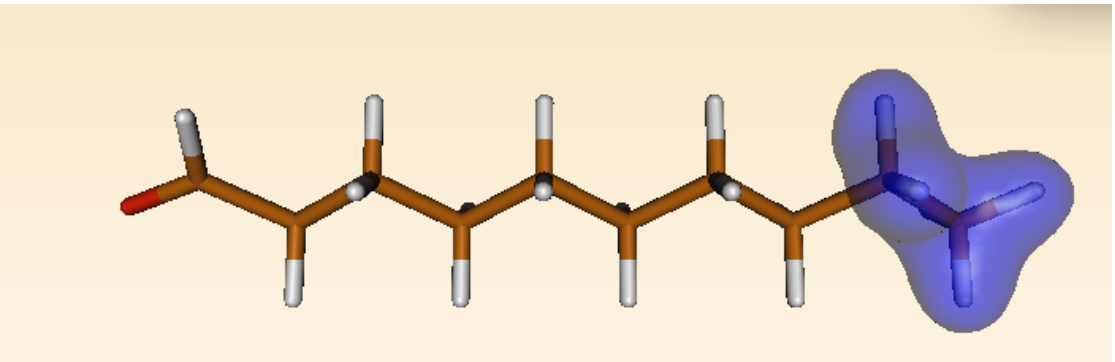

Figure 3: CCS space of decanal.

bigger space in Figure 2 shows the part treated with CC2. The atoms that are furthest from the active space are in this example treated with CCS. The figures give a picture of how the system is divided into spaces and how these are based on the relevance of each atom to the specific calculations. They also show how the highest level of theory is only applied to a small part of the system and why there will be a reduction in computational cost. Cholesky decomposition is now widely used to decrease scaling in coupled cluster calculations [12, 14, 15, 34]. The reason Cholesky decomposition is such a useful tool in computational chemistry is the saving that results from being able to remove zero or small eigenvalues without calculating the whole matrix. An illustrative example is a two electron integral matrix, which would scale as N^4, where N is the number of orbitals. The number of non-zero eigenvalues, however, scales as N, leading to a considerable reduction in scaling for large basis sets [35].

2.2.2 The ECC2 Model

In the ECC2 model the system is divided into two levels. CCSD is used on the part that is to be treated most accurately (the active space), and CC2 is used on the rest of the system (inactive space). CC2 is also used on the excitations that are semi-external to the active space, i.e. from active to inactive or from inactive to active space. Using a small active space, the computational complexity should scale as CC2 while, as shown by Myhre et al., give results closer to or as good

as CCSD. Eq. (2.17) shows how the energy of the ground state is computed [9], where T and S come from the splitting of the cluster operator, X

$$X = S + T \tag{2.16}$$

In Eq. (2.16) S corresponds to the excitations external and semi-external to the active space, treated with the CC2 model and T to the excitations in the active space, treated with the CCSD model.

$$E_0 = \langle HF | H_0 \exp(T + S) | HF \rangle \tag{2.17}$$

Because all single excitations are treated to infinite order in both CC2 and CCSD combining Eq. (2.11) and (2.16) gives

$$X = T_1 + T_2 + S_2 = \sum_{\mu_1} t_{\mu_1} \tau_{\mu_1} + \sum_{\mu_2^T} t_{\mu_2^T} \tau_{\mu_2^T} + \sum_{\mu_2^S} t_{\mu_2^S} \tau_{\mu_2^S} \tag{2.18}$$

where μ_1 refers to single excitations and μ_2^T and μ_2^S refer to double excitations treated with CCSD and CC2 theory respectively. The ECC2 model does not include triple or higher excitations, and the cluster operator has thus been truncated at double excitations.

2.3 Response Theory

Response Theory is used to describe a molecular system's response to external potentials such as electromagnetic fields [17]. Assuming that the external potentials are weak compared to the internal ones, they can be regarded as perturbations of the isolated system. As this is the case for electronic excitations, this method can be used and it is refered to as the quasienergy (QE) method. In practice, only the ground state wave function needs to be calculated. Properties of excited states can then be extracted by adding the time dependent perturbation, V^t, as shown in Eq. (2.20), without explicitly computing the excited state's wave function. The ground state is found from the time-independent Schrödinger equation, Eq. (2.19), where H_0 is the hamiltonian for the ground state and E_0 the corresponding energy.

$$H_0|HF\rangle = E_0|HF\rangle \tag{2.19}$$

$$H = H_0 + V^t \tag{2.20}$$

The computational advantage of not having to calculate all excited wave functions explains why response theory is commonly used in computational chemistry [36, 37]. To obtain the excited state properties the general response equation needs to be solved.

$$[\mathcal{H} - \omega\mathcal{S}]\,\lambda^{(n)}(\omega) = -\mathcal{V}^{(n)}(\omega) \tag{2.21}$$

In Eq. (2.21) the unkonwn quantity is the vector $\lambda^{(n)}(\omega)$ while the matrices $\mathcal{H}$ and $\mathcal{S}$ only depend on the unperturbed ground state wave function. Depending on the approximation method used, the vectors and matrices in Eq. (2.21) will have different forms, but the unknown vector $\lambda^{(n)}(\omega)$ always contains the nth-order wave function parameter. The vector $\mathcal{V}^{(n)}(\omega)$ depends on the lower-order wave function parameters up to $\lambda^{(n-1)}$ in addition to one or more perturbation operators.

2.3.1 Linear Response Function

The exact linear response function shown in Eq. (2.22) is singular at the molecular excitation energies [17].

$$\langle\langle A, B\rangle\rangle_\omega = \sum_{k\neq 0}\left(\frac{\langle 0|A|k\rangle\langle k|B|0\rangle}{\omega - \omega_{k_0}} - \frac{\langle 0|B|k\rangle\langle k|A|0\rangle}{\omega + \omega_{k_0}}\right) \tag{2.22}$$

The fact that the excitation energies give a singular linear response function is equivalent to them occuring at $\pm\omega_{k_0}$. This is used to find the excitation energies when approximate methods such as CC are implemented. The way this is done is by identifying the frequencies for which Eq. (2.21) is singular. The use of response theory greatly reduces the computational cost compared to calculating excited state wave functions explicitly. The residue of the response function at ω_{k_0} is the product of the left and right first-order transition matrix elements.

$$\lim_{\omega\to\omega_k}(\omega-\omega_k)\,\langle\langle A,B\rangle\rangle_\omega = \langle 0|A|k\rangle\langle k|B|0\rangle \tag{2.23}$$

$$\lim_{\omega\to-\omega_k}(\omega+\omega_k)\,\langle\langle A,B\rangle\rangle_\omega = -\langle 0|B|k\rangle\langle k|A|0\rangle \tag{2.24}$$

Even though $\langle k|A|0\rangle = \langle 0|A|k\rangle^*$ in exact theory, it is convenient for comparison with CC response theory to express the residues in the following way.

$$\lim_{\omega\to\omega_k}(\omega-\omega_k)\,\langle\langle A,B\rangle\rangle_\omega = \frac{1}{2}\left[\langle 0|A|k\rangle\langle k|B|0\rangle + \Big(\langle 0|B|k\rangle\langle k|A|0\rangle\Big)^*\right] \tag{2.25}$$

$$\lim_{\omega\to-\omega_k}(\omega+\omega_k)\,\langle\langle A,B\rangle\rangle_\omega = -\frac{1}{2}\left[\langle 0|B|k\rangle\langle k|A|0\rangle + \Big(\langle 0|A|k\rangle\langle k|B|0\rangle\Big)^*\right] \tag{2.26}$$

2.4 MLCC Response Theory

Using time-dependent perturbation theory, the linear response function for both CC2 and CCSD can be derived [38, 39, 40]. In the derivation of the linear response function for the ECC2 model, Myhre et al. used the Quasi-Energy (QE) Lagrangian method [41] where the Hamiltonian is divided into a ground state, H_0 and a time-dependent perturbation, V^t as shown in Eq. (2.20). The QE Lagrangian of the ECC2 model [42] is given in Eq. (2.29) where

$$\langle\tilde{\Lambda}| = \langle HF| + \sum_\mu \bar{t}_\mu(t)\langle\mu|\exp\left(-T(t)\right) \tag{2.27}$$

$$|\widetilde{CC}(t)\rangle = \exp\left(T(t)+S(t)\right)|HF\rangle \tag{2.28}$$

$$
\begin{aligned}
L(t) &= Re\left(\langle\tilde{\Lambda}\left[H_0 + V^t - i\frac{d}{dt}\right]|\widetilde{CC}(t)\rangle\right) \\
&= \langle HF|H\exp(T+S)|HF\rangle \\
&+ \sum_{\mu_1}\bar{t}_{\mu_1}\left(\langle\mu_1|\hat{H} + [\hat{H}, X_2]|HF\rangle - i\frac{dt_{\mu_1}}{dt}\right) \\
&+ \sum_{\mu_2^T}\bar{t}_{\mu_2^T}\left(\langle\mu_2^T|\hat{H} + [\hat{H}, X_2] + \frac{1}{2}[[\hat{H}, X_2], X_2]|HF\rangle - i\frac{dt_{\mu_2^T}}{dt}\right) \\
&+ \sum_{\mu_2^S}\bar{t}_{\mu_2^S}\left(\langle\mu_2^S|[\hat{F} + \hat{V}, S_2] + \hat{H} + [\hat{H}, T_2]|HF\rangle - i\frac{dt_{\mu_2^S}}{dt}\right)
\end{aligned}
\tag{2.29}
$$

To simplify the Lagrangian, the T_1 transformed Hamiltonian, $\hat{H}$, is used. $\hat{H}$ has the same structure as H, but with different coeffiecients.

$$
\hat{H} = \exp(-T_1)H\exp(T_1) \tag{2.30}
$$

The response function is found by derivating the QE Lagrangian with respect to the strength parameters ϵ_A and ϵ_B that are given by the first order amplitudes, $t_\mu^{(1)}(t)$.

$$
t_\mu^{(1)}(t) = \sum_{j=-N}^{N}\sum_{A} t_\mu^A(\omega_j)\epsilon_A(\omega_j)\exp(-i\omega_j t) \tag{2.31}
$$

For the ECC2 model, the linear response function [42] is given in Eq. (2.34), where $\hat{A}$ is the T_1 transformed perturbation operator, A, and

$$
\begin{aligned}
&P\left(A\left(-\omega_i\right), B\left(\omega_i\right)\right) f\left(A\left(-\omega_i\right), B\left(\omega_i\right)\right) = \\
&f\left(A\left(-\omega_i\right), B\left(\omega_i\right)\right) + f\left(B\left(\omega_i\right), A\left(-\omega_i\right)\right)
\end{aligned}
\tag{2.32}
$$

$$
M^{\pm\omega} f^{AB}(\omega_A, \omega_B) = f^{AB}(\omega_A, \omega_B) + [f^{AB}(-\omega_A, -\omega_B)]^* \tag{2.33}
$$

$$
\begin{aligned}
&\langle\langle A,B\rangle\rangle_{\omega i} = \frac{\partial\{L^{(2)}\}_\tau}{\partial\epsilon_A(-\omega_i)\partial\epsilon_B(\omega_i)} \\
=&\frac{1}{2}M^{\pm\omega}P\left(A\left(-\omega_i\right),B\left(\omega_i\right)\right) \\
&\Bigg\{\langle HF|[\hat{A},T_1^{(B)}]+\frac{1}{2}[[\hat{H}_0,T_1^{(A)}],T_1^{(B)}]|HF\rangle \\
&+\sum_{\mu_1}\bar{t}^{(0)}_{\mu_1}\langle\mu_1|[\hat{A},X^{(B)}]+\frac{1}{2}[[\hat{H}_0,X^{(A)}],X^{(B)}]|HF\rangle \\
&+\sum_{\mu_2^T}\bar{t}^{(0)}_{\mu_2^T}\langle\mu_2^T|[\hat{A},X_2^{(B)}]+\frac{1}{2}[[\hat{H}_0,T_1^{(A)}],T_1^{(B)}] \\
&+[[\hat{A},T_1^{(B)}],X_2^{(0)}]+[[\hat{H}_0,T_1^{(A)}],X_2^{(B)}] \\
&+\frac{1}{2}[[[\hat{H}_0,T_1^{(A)}],T_1^{(B)}],X_2^{(0)}]+\frac{1}{2}[[\hat{H}_0,X_2^{(A)}],X_2^{(B)}]|HF\rangle \\
&+\sum_{\mu_2^S}\bar{t}^{(0)}_{\mu_2^S}\langle\mu_2^S|[\hat{A},X_2^{(B)}]+\frac{1}{2}[[\hat{H}_0,T_1^{(A)}],T_1^{(B)}]+[[\hat{A},T_1^{(B)}],T_2^{(0)}] \\
&+[[\hat{H}_0,T_1^{(A)}],T_2^{(B)}]+\frac{1}{2}[[[\hat{H}_0,T_1^{(A)}],T_1^{(B)}],T_2^{(0)}]|HF\rangle\Bigg\}
\end{aligned}
\tag{2.34}
$$

The operators A and B are found from the Fourier transform of the perturbation operator.

$$
V^t = \sum_{j=-N}^{N}\sum_{A} A\epsilon_A(\omega_j)e^{(-i\omega_j t)} \tag{2.35}
$$

The cluster operator in Eq. (2.29) and (2.34) is given by the product of the excitation operator, τ_μ, and the amplitude of the excitation, $t_\mu\left(t\right)$, as shown in Eq. (2.11). In Eq. (2.34) all single excitations $\langle\mu_1|$, are treated to infinite order and are therefore gathered, i.e. they are treated the same way for CC2 and CCSD. Double excitations are treated differently, and this is why we have two sums; one over all excitations treated with CCSD, i.e. the $\langle\mu_2^T|$ term and one over all excitations treated with CC2, which would be the $\langle\mu_2^S|$ term. It should also be noted that the T_1 transformation will not affect all of the terms, because the commutators arising from the transformation do not contribute if they are of a higher order than the

excitation in question.

2.5 Derivation of the Transition Moment for ECC2

When the excitation energies have been calculated, the residue of the linear response function is used to identify the transition moments. Because the transition moment dictates whether or not a specific excitation is allowed [16], it is a highly useful property to compute. For the transitions that are allowed, the transition moment gives information on the probability of it occuring. This is not the only reason one is interested in the transition moment's properties. The square of the transition moment, i.e. the transition amplitude, is proportional to the intensity of the transition. In general, the greater the transition moment of a given transition, the more intense spectral lines will be. For the derivation of the transition amplitude, it is convenient to have Eq. (2.34) expressed in a more compact way. This can be done using Eq. (2.16) and (2.11). First we create a vector, $\boldsymbol{C}^{(O)}$, of all the terms containing the operators A and B and a matrix, $\boldsymbol{\mathcal{F}}$, containing the hamiltonian part. Then the amplitudes, $\boldsymbol{t}$, can be pulled out of both $\boldsymbol{C}^{(O)}$ and $\boldsymbol{\mathcal{F}}$, giving two amplitude vectors, $\boldsymbol{t}^{(A)}(-\omega)$ and $\boldsymbol{t}^{(B)}(\omega)$. The response equation can be expressed as a vector product as shown in Eq. (2.38). Inspecting Eq. (2.34) the components of Eq. (2.38) can be identified as

$$\boldsymbol{C}^{(B)} = \tag{2.36}$$
$$\begin{pmatrix} \sum_\nu \Big\{ \langle HF|[\hat{B},\tau_{\nu_1}] + \sum_{\mu_1} \bar{t}^{(0)}_{\mu_1} \langle \mu_1|[\hat{B},\tau_{\nu_1}] + \sum_{\mu_2^S} \bar{t}^{(0)}_{\mu_2^S} \langle \mu_2^S|[[\hat{B},\tau_{\nu_1}],T_2^{(0)}] \\ + \sum_{\mu_2^T} \bar{t}^{(0)}_{\mu_2^T} \langle \mu_2^T|[[\hat{B},\tau_{\nu_1}],X_2^{(0)}]|HF\rangle \Big\} \\ \sum_{\mu_1} \bar{t}^{(0)}_{\mu_1} \langle \mu_1|[\hat{B},\tau_{\nu_2^S}] + \sum_{\mu_2^S} \bar{t}^{(0)}_{\mu_2^S} \langle \mu_2^S|[\hat{B},\tau_{\nu_2^S}] + \sum_{\mu_2^T} \bar{t}^{(0)}_{\mu_2^T} \langle \mu_2^T|[\hat{B},\tau_{\nu_2^S}]|HF\rangle \\ \sum_{\mu_1} \bar{t}^{(0)}_{\mu_1} \langle \mu_1|[\hat{B},\tau_{\nu_2^S}] + \sum_{\mu_2^S} \bar{t}^{(0)}_{\mu_2^S} \langle \mu_2^S|[\hat{B},\tau_{\nu_2^T}] + \sum_{\mu_2^T} \bar{t}^{(0)}_{\mu_2^T} \langle \mu_2^T|[\hat{B},\tau_{\nu_2^T}]|HF\rangle \end{pmatrix}^T$$

$$\boldsymbol{\mathcal{F}} = \begin{pmatrix}
\begin{array}{c}
\langle HF|[[\hat{H}_0,\tau_{\gamma_1}],\tau_{\nu_1}]|HF\rangle \\
+\sum_{\mu_1}\bar{t}^{(0)}_{\mu_1}\langle\mu_1|[[\hat{H}_0,\tau_{\gamma_1}],\tau_{\nu_1}]|HF\rangle \\
+\sum_{\mu_2^T}\bar{t}^{(0)}_{\mu_2^T}\langle\mu_2^T|\Big([[\hat{H}_0,\tau_{\gamma_1}],\tau_{\nu_1}] \\
+[[[\hat{H}_0,\tau_{\gamma_1}],\tau_{\nu_1}],X_2^{(0)}]\Big)|HF\rangle \\
+\sum_{\mu_2^S}\bar{t}^{(0)}_{\mu_2^S}\langle\mu_2^S|\Big([[\hat{H}_0,\tau_{\gamma_1}],\tau_{\nu_1}] \\
+[[[\hat{H}_0,\tau_{\gamma_1}],\tau_{\nu_1}],T_2^{(0)}]\Big)|HF\rangle
\end{array} &
\begin{array}{c}
\sum_{\mu_1}\bar{t}^{(0)}_{\mu_1}\langle\mu_1|[[\hat{H}_0,\tau_{\gamma_1}],\tau_{\nu_2^T}]|HF\rangle \\
+\sum_{\mu_2^T}\bar{t}^{(0)}_{\mu_2^T}\langle\mu_2^T|[[\hat{H}_0,\tau_{\gamma_1}],\tau_{\nu_2^T}]|HF\rangle \\
+\sum_{\mu_2^S}\bar{t}^{(0)}_{\mu_2^S}\langle\mu_2^S|[[\hat{H}_0,\tau_{\gamma_1}],\tau_{\nu_2^T}]|HF\rangle
\end{array} &
\begin{array}{c}
\sum_{\mu_1}\bar{t}^{(0)}_{\mu_1}\langle\mu_1|[[\hat{H}_0,\tau_{\gamma_1}],\tau_{\nu_2^S}]|HF\rangle \\
+\sum_{\mu_2^T}\bar{t}^{(0)}_{\mu_2^T}\langle\mu_2^T|[[\hat{H}_0,\tau_{\gamma_1}],\tau_{\nu_2^S}]|HF\rangle
\end{array} \\
\begin{array}{c}
\sum_{\mu_1}\bar{t}^{(0)}_{\mu_1}\langle\mu_1|[[\hat{H}_0,\tau_{\gamma_2^T}],\tau_{\nu_1}]|HF\rangle \\
+\sum_{\mu_2^T}\bar{t}^{(0)}_{\mu_2^T}\langle\mu_2^T|[[\hat{H}_0,\tau_{\gamma_2^T}],\tau_{\nu_1}]|HF\rangle \\
+\sum_{\mu_2^S}\bar{t}^{(0)}_{\mu_2^S}\langle\mu_2^S|[[\hat{H}_0,\tau_{\gamma_2^T}],\tau_{\nu_1}]|HF\rangle
\end{array} &
\sum_{\mu_2^T}\bar{t}^{(0)}_{\mu_2^T}\langle\mu_2^T|[[\hat{H}_0,\tau_{\gamma_2^T}],\tau_{\nu_2^T}]|HF\rangle &
\sum_{\mu_2^T}\bar{t}^{(0)}_{\mu_2^T}\langle\mu_2^T|[[\hat{H}_0,\tau_{\gamma_2^T}],\tau_{\nu_2^S}]|HF\rangle \\
\begin{array}{c}
\sum_{\mu_1}\bar{t}^{(0)}_{\mu_1}\langle\mu_1|[[\hat{H}_0,\tau_{\gamma_2^S}],\tau_{\nu_1}]|HF\rangle \\
+\sum_{\mu_2^T}\bar{t}^{(0)}_{\mu_2^T}\langle\mu_2^T|[[\hat{H}_0,\tau_{\gamma_2^S}],\tau_{\nu_1}]|HF\rangle
\end{array} &
\sum_{\mu_2^T}\bar{t}^{(0)}_{\mu_2^T}\langle\mu_2^T|[[\hat{H}_0,\tau_{\gamma_2^S}],\tau_{\nu_2^T}]|HF\rangle &
\sum_{\mu_2^T}\bar{t}^{(0)}_{\mu_2^T}\langle\mu_2^T|[[\hat{H}_0,\tau_{\gamma_2^S}],\tau_{\nu_2^S}]|HF\rangle
\end{pmatrix}$$

$$\boldsymbol{t}^{(A)}(-\omega)\begin{pmatrix} t^{(A)}_{\nu_1}(-\omega) \\ \\ t^{(A)}_{\nu_2^S}(-\omega) \\ \\ t^{(A)}_{\nu_2^T}(-\omega) \end{pmatrix} \tag{2.37}$$

$$\langle\langle A, B\rangle\rangle_\omega = \sum_\nu C^{(A)}_\nu t^{(B)}_\nu(\omega) + \sum_\gamma \left(C^{(B)}_\gamma + \sum_\nu \mathcal{F}_{\gamma\nu} t^{(B)}_\nu(\omega) \right) t^{(A)}_\gamma(-\omega) \tag{2.38}$$

The CC response equation, Eq. (2.39) can now be compared to the exact response equation, Eq. (2.21). In Eq. (2.39) we have the unkonwn amplitudes, $\boldsymbol{t}^{(B)}(\omega)$, the unit matrix, $\mathbf{1}$, the matrix $\boldsymbol{A}$ that is dependent on the ground state of the system and the vector $\boldsymbol{\xi}^B$ that depends on the perturbation and the 0^{th} order amplitude.

$$\boldsymbol{t}^{(B)}(\omega) = (\omega\mathbf{1} - \boldsymbol{A})^{-1}\boldsymbol{\xi}^B \tag{2.39}$$

$\boldsymbol{A}$ is the ECC2 Jacobian, Eq. (2.41) and

$$\boldsymbol{\xi}^B = \begin{pmatrix} \langle\mu_1|\hat{B} + [\hat{B}, X_2^{(0)}]|HF\rangle \\ \langle\mu_2^T[\hat{B}, X_2^{(0)}]|HF\rangle \\ \langle\mu_2^S[\hat{B}, X_2^{(0)}]|HF\rangle \end{pmatrix} \tag{2.40}$$

$$\boldsymbol{A}_{ECC2} = \tag{2.41}$$
$$\begin{pmatrix} \langle\mu_1|[\hat{H}_0 + [\hat{H}_0, X_2^{(0)}]\tau_{\nu_1}]|HF\rangle & \langle\mu_1|[\hat{H}_0, \tau_{\nu_2^T}]|HF\rangle & \langle\mu_1|[\hat{H}_0, \tau_{\nu_2^S}]|HF\rangle \\ \langle\mu_2^T|[\hat{H}_0 + [\hat{H}_0, X_2^{(0)}]\tau_{\nu_1}]|HF\rangle & \langle\mu_2^T|[\hat{H}_0 + [\hat{H}_0, X_2^{(0)}]\tau_{\nu_2^T}]|HF\rangle & \langle\mu_2^T|[\hat{H}_0 + [\hat{H}_0, X_2^{(0)}]\tau_{\nu_2^S}]|HF\rangle \\ \langle\mu_2^S|[\hat{H}_0 + [\hat{H}_0, T_2^{(0)}]\tau_{\nu_1}]|HF\rangle & \langle\mu_2^S|[\hat{H}_0, \tau_{\nu_2^T}]|HF\rangle & \langle\mu_2^S|[F, \tau_{\nu_2^S}]|HF\rangle \end{pmatrix}$$

The excitation energies are found by determining the eigenvalues of the Jacobian matrix, $\boldsymbol{A}$, and this has been done by Myhre et al. To determine the transition moments, the frequencies for which Eq. (2.39) is singular need to be determined. As the Jacobian is nonsymmetric it has both right and left eigenstates and a similarity transformation [16] can be used to diagonalize it:

$$(\boldsymbol{LAR})_{nm} = \delta_{nm}\omega_n \tag{2.42}$$

where the n^{th} row column of $\boldsymbol{R}$ is assumed to be the right eigenvector of $\boldsymbol{A}$, $|k\rangle$ and the n^{th} row of $\boldsymbol{L}$ the left eigenvector of $\boldsymbol{A}$, $\langle k|$ corresponding to the eigenvalue ω_n. The excitation and deexcitation operators can now be expressed as diagonal representations, τ_n and $\tau_n^\dagger$, using

$$\tau_n = \sum_\nu \tau_\nu R_{\nu n} \tag{2.43}$$

$$\tau_n^\dagger = \sum_\nu L_{n\nu}\tau_\nu^\dagger \tag{2.44}$$

where $L_{n\nu}$ is the element in the n^{th} row and ν^{th} column of $\boldsymbol{L}$. Using the diagnoal representations Eq. (2.38) may now be written as

$$\langle\langle A, B\rangle\rangle_\omega = \sum_n C_n^{(A)} t_n^{(B)}(\omega) + \sum_m \left(C_n^{(B)} + \sum_n \mathcal{F}_{mn} t_n^{(B)}(\omega) \right) t_m^{(A)}(-\omega) \tag{2.45}$$

where the excitation operators in Eq. (2.34) have been replaced with the diagonal representations. The represenation of the vector $\boldsymbol{\xi}^{(A)}$ can also be changed from $\xi_\mu^{(A)}$ where

$$\mu = \begin{pmatrix} \mu_1 \\ \mu_2^S \\ \mu_2^T \end{pmatrix} \tag{2.46}$$

to $\xi_n^{(A)}$, using the left eigenvectors of the Jacobian, $\boldsymbol{L}$ and we now have that

$$\xi_n^{(A)} = \sum_\mu L_{n\mu}\xi_\mu^{(A)} \tag{2.47}$$

Writing Eq. (2.39) on component form using the left eigenvector from the diagonal representation of $\boldsymbol{A}$ and $\boldsymbol{\xi}^{(A)}$ we get

$$t_n^{(A)}(-\omega) = -(\omega + \omega_n)^{-1}\xi_n^{(A)} \tag{2.48}$$

Now this can be substituted into Eq. (2.45) and we end up with an expression similar to that of Christiansen et al. [43].

$$\langle\langle A, B\rangle\rangle_\omega = \frac{1}{2}M^{\pm\omega}\left(\sum_n \frac{C_n^{(A)}\xi_n^{(B)}}{(\omega - \omega_n)} - \sum_m \frac{\xi_m^{(A)}C_m^{(B)}}{(\omega + \omega_m)} - \sum_{mn} \frac{\xi_m^{(A)}\mathcal{F}_{mn}\xi_n^{(B)}}{(\omega + \omega_m)(\omega - \omega_n)}\right) \tag{2.49}$$

Comparing Eq. (2.49) to Eq. (2.22), we see that the $\boldsymbol{\mathcal{F}}$ term looks like it comes in addition to exact theory. As a rather uncommon feature for nonvariational approaches, the coupled cluster $\boldsymbol{\mathcal{F}}$ term does not change the pole structure, and therefore allows for a nonambiguous determination of poles and residues. In fact, Christiansen et al.[43] point out that the $\boldsymbol{\mathcal{F}}$ term arises naturally because of the nonvariational exponential parametrization, the same way as it enters in time-independent energy derivatives. The residues at the poles of the response function at $\pm\omega_k$, i.e. $\lim_{\omega\to\omega_k}(\omega - \omega_k)\langle\langle A, B\rangle\rangle_\omega$ and $\lim_{\omega\to-\omega_k}(\omega + \omega_k)\langle\langle A, B\rangle\rangle_\omega$, are used to determine the transition moment properties. From Eq. (2.49) one can see that the component form of the two residues become

$$\lim_{\omega\to\omega_k}(\omega-\omega_k)\langle\langle A,B\rangle\rangle_\omega =$$
$$\frac{1}{2}\left[\left(C_k^{(A)}-\sum_m\frac{\xi_m^{(A)}\mathcal{F}_{mk}}{\omega_k+\omega_m}\right)\xi_k^{(B)}-\left(\left(C_k^{(B)}+\sum_n\frac{\mathcal{F}_{kn}\xi_n^{(B)}}{\omega_k+\omega_n}\right)\xi_k^{(A)}\right)^*\right] \tag{2.50}$$

$$\lim_{\omega\to-\omega_k}(\omega+\omega_k)\langle\langle A,B\rangle\rangle_\omega =$$
$$\frac{1}{2}\left[\left(-C_k^{(B)}+\sum_n\frac{\xi_n^{(B)}\mathcal{F}_{kn}}{\omega_k+\omega_n}\right)\xi_k^{(A)}+\left(\left(C_k^{(A)}+\sum_m\frac{\mathcal{F}_{mk}\xi_m^{(A)}}{\omega_k+\omega_m}\right)\xi_k^{(B)}\right)^*\right] \tag{2.51}$$

As we do not need a complete diagonalization it is more common to express the transition moments using both the diagonal and elementary basis [38, 43]. This is how they are computed in DALTON [44] and using Eq. (2.43) and Eq. (2.54) the implementation of the ECC2 model to calculate transition moments becomes more transparent. In Eq (2.52) and (2.53) we have also used the fact that the $\boldsymbol{\mathcal{F}}$ matrix is symmetric, i.e. $\mathcal{F}_{kn}=\mathcal{F}_{nk}$.

$$\lim_{\omega\to\omega_k}(\omega-\omega_k)\langle\langle A,B\rangle\rangle_\omega = \tag{2.52}$$
$$\frac{1}{2}\sum_\nu\left[\left(C_\nu^{(A)}+\sum_\gamma t_\gamma^{(A)}\mathcal{F}_{\gamma\nu}\right)R_{\nu k}\xi_k^{(B)}-\left(\left(C_\gamma^{(B)}-\sum_\gamma t_\gamma^{(B)}\mathcal{F}_{\gamma\nu}\right)R_{\nu k}\xi_k^{(A)}\right)^*\right]$$

$$\lim_{\omega\to-\omega_k}(\omega+\omega_k)\langle\langle A,B\rangle\rangle_\omega = \tag{2.53}$$
$$\frac{1}{2}\sum_\nu\left[\left(-C_\gamma^{(B)}-\sum_\gamma t_\gamma^{(B)}\mathcal{F}_{\gamma\nu}\right)R_{\nu k}\xi_k^{(A)}+\left(\left(C_\nu^{(A)}-\sum_\gamma t_\gamma^{(A)}\mathcal{F}_{\gamma\nu}\right)R_{\nu k}\xi_k^{(B)}\right)^*\right]$$

$$\sum_m\frac{\xi_m^{(A)}\mathcal{F}_{mk}}{\omega_k+\omega_m}=-\sum_\gamma t_\gamma^{(A)}(-\omega_k)\mathcal{F}_{\gamma k} \tag{2.54}$$

Now introducing the CC left and right transition matrix elements, $\langle k|A|0\rangle$ and

$\langle 0|B|k\rangle$, the resemblance to exact theory becomes more apparent.

$$\langle k|A|0\rangle = \sum_{\mu} L_{k\mu}\xi_{\mu}^{(A)} \tag{2.55}$$

$$\langle 0|B|k\rangle = \sum_{\nu} C_{\nu}^{(B)} R_{\nu k} + \sum_{\nu\gamma} t^{(B)} \mathcal{F}_{\gamma\nu} R_{\nu k} \tag{2.56}$$

The ECC2 residues do, in fact, look quite similar to the exact theory, using the relations in Eq. (2.55) and (2.56). A difference from the transition matrix elements in exact theory is that in CC $\langle k|A|0\rangle \neq \langle 0|A|k\rangle^*$, which is a consequence of using the quasienergy response method [43]. This is the motivation for introducing the symmetrization with respect to complex conjugation and sign reversal of the frequencies in Eq. (2.25) and (2.26). As the excitaion energies are calculated by solving the eigenvalue problem $\boldsymbol{A}R_k = \omega_k R_k$ or $L_k\boldsymbol{A} = \omega_k L_k$, either right or left eigenvectors can be used. For the transition moments, however, both left and right eigenvectors are needed.

3 Implementation

The DALTON 2013 software package [44] is used for the implementation of the ECC2 model. As the $\boldsymbol{C}^{(\hat{O})}$ vectors are a part of the excitation energy calculation, the term that we will focus on in this section is the one containing the $\boldsymbol{\mathcal{F}}$ matrix. To test the ECC2 model the already embedded CC2 and CCSD models are combined and we need to look at the individual $\boldsymbol{\mathcal{F}}$ to find the most efficient way to do this. The ECC2 $\boldsymbol{\mathcal{F}}$ matrix therefore needs to be viewed as a sum of the part treated with CCSD, $\boldsymbol{\mathcal{F}}^{CCSD}$, and the part treated with CC2, $\boldsymbol{\mathcal{F}}^{CC2}$ as in Eq. (3.1), where the eigenvectors, $\boldsymbol{R}_i$ and amplitudes $\boldsymbol{t}_i^{(A)}(-\omega)$ as well as the multipliers, $\bar{\boldsymbol{t}}^{(0)}$, and the zero order amplitudes, $\boldsymbol{X}^{(0)}$ are manipulated to obtain the desired result.

$$\boldsymbol{t}^{(A)}(-\omega)\boldsymbol{\mathcal{F}}\boldsymbol{R} = \sum_i \boldsymbol{t}_i^{(A)}(-\omega)\boldsymbol{\mathcal{F}}^{CCSD}{}_i\boldsymbol{R} + \sum_j \boldsymbol{t}_j^{(A)}(-\omega)\boldsymbol{\mathcal{F}}^{CC2}{}_j\boldsymbol{R} \tag{3.1}$$

The response equation for CC2 is given by Christiansen et al. [10].

$$\begin{aligned}
&\langle\langle A, B\rangle\rangle_\omega = P\big(A(-\omega), B(\omega)\big) \\
&\times \Bigg\{ \langle HF|[A, T_1^B(\omega)] + \frac{1}{2}[[H_0, T_1^A(-\omega)], T_1^B(\omega)]|HF\rangle \\
&+ \sum_{\mu_1} \bar{t}_{\mu_1}^{(0)} \langle \mu_1|[A, T^B(\omega)] + \frac{1}{2}[[H_0, T_1^A(-\omega)], T_1^B(\omega)]|HF\rangle \\
&+ \sum_{\mu_2} \bar{t}_{\mu_2}^{(0)} \langle \mu_2|[A, T_2^B(\omega)] + [[A, T_1^B], T_2^{(0)}] \\
&+ \frac{1}{2}[[H_0, T_1^A(-\omega)], T_1^B(\omega)]|HF\rangle \Bigg\}
\end{aligned} \tag{3.2}$$

After using the permutation operator and following the same steps as for the ECC2 $\mathcal{F}$ matrix we find the $\boldsymbol{\mathcal{F}}^{CC2}$ matrix.

$$\boldsymbol{\mathcal{F}}^{CC2} = \begin{pmatrix} \langle HF|[[H_0,\tau_{\gamma_1}],\tau_{\nu_1}]|HF\rangle & \sum_{\mu_1} \bar{t}^{(0)}_{\mu_1}\langle\mu_1|[[\hat{H}_0,\tau_{\gamma_1}],\tau_{\nu_2}]|HF\rangle \\ +\sum_{\mu_1} \bar{t}^{(0)}_{\mu_1}\langle\mu_1|[[\hat{H}_0,\tau_{\gamma_1}],\tau_{\nu_1}]|HF\rangle & \\ +\sum_{\mu_2} \bar{t}^{(0)}_{\mu_2}\langle\mu_2|[[\hat{H}_0,\tau_{\gamma_1}],\tau_{\nu_1}]|HF\rangle & \\ \sum_{\mu_1} \bar{t}^{(0)}_{\mu_1}\langle\mu_1|[[\hat{H}_0,\tau_{\gamma_2}],\tau_{\nu_1}]|HF\rangle & 0 \end{pmatrix}$$

Splitting the second order excitations into S and T gives a three dimensional matrix. This makes it easier to compare it to the ECC2 $\boldsymbol{\mathcal{F}}$ matrix.

$$\boldsymbol{\mathcal{F}}^{CC2} = \begin{pmatrix} \langle HF|[[H_0,\tau_{\gamma_1}],\tau_{\nu_1}]|HF\rangle \\ +\sum_{\mu_1} \bar{t}^{(0)}_{\mu_1}\langle\mu_1|[[\hat{H}_0,\tau_{\gamma_1}],\tau_{\nu_1}]|HF\rangle \\ +\sum_{\mu_2^T} \bar{t}^{(0)}_{\mu_2^T}\langle\mu_2^T|[[\hat{H}_0,\tau_{\gamma_1}],\tau_{\nu_1}]|HF\rangle \\ +\sum_{\mu_2^S} \bar{t}^{(0)}_{\mu_2^S}\langle\mu_2^S|[[\hat{H}_0,\tau_{\gamma_1}],\tau_{\nu_1}]|HF\rangle & \sum_{\mu_1} \bar{t}^{(0)}_{\mu_1}\langle\mu_1|[[\hat{H}_0,\tau_{\gamma_1}],\tau_{\nu_2^T}]|HF\rangle & \sum_{\mu_1} \bar{t}^{(0)}_{\mu_1}\langle\mu_1|[[\hat{H}_0,\tau_{\gamma_1}],\tau_{\nu_2^S}]|HF\rangle \\ \sum_{\mu_1} \bar{t}^{(0)}_{\mu_1}\langle\mu_1|[[\hat{H}_0,\tau_{\gamma_2^T}],\tau_{\nu_1}]|HF\rangle & 0 & 0 \\ \sum_{\mu_1} \bar{t}^{(0)}_{\mu_1}\langle\mu_1|[[\hat{H}_0,\tau_{\gamma_2^S}],\tau_{\nu_1}]|HF\rangle & 0 & 0 \end{pmatrix}$$

The CCSD response equation, given by Koch et al. [40], is

$$\begin{aligned}\langle\langle A, B\rangle\rangle_\omega = &\sum_\gamma \langle\Lambda|[A,\tau_\gamma]|CC\rangle t_\gamma^{(B)}(\omega) \\ &+ \sum_\nu \Big\{ \langle\Lambda|[B,\tau_\nu|CC\rangle \\ &+ \sum_\gamma \langle\Lambda|[[H,\tau_\gamma],\tau_\nu]|CC\rangle t_\nu^B(\omega) \Big\} t_\gamma^A(-\omega)\end{aligned} \tag{3.3}$$

In Eq. (3.3) $\langle\Lambda| = \langle HF| + \sum_\mu \bar{t}_\mu^{(0)}\langle\mu|\exp(-X)$, where X is the CC operator. The CC wave function is given by $|CC\rangle = \exp(X)|HF\rangle$. Now using the fact that

$$\exp(-X)H\exp(X) = H + [H,X] + \frac{1}{2}[[H,X],X] + \frac{1}{3!}[[[H,X],X],X] + \cdots \tag{3.4}$$

and that

$$\langle HF| = \langle HF|\exp(-X) \tag{3.5}$$

The $\boldsymbol{\mathcal{F}}^{CCSD}$ matrix can be derived.

$$\boldsymbol{\mathcal{F}}^{CCSD} = \begin{pmatrix} \langle HF|[[H_0,\tau_{\gamma_1}],\tau_{\nu_1}] + [[[H_0,\tau_{\gamma_1}],\tau_{\nu_1}],X]|HF\rangle \\ + \sum_{\mu_1} \bar{t}^{(0)}_{\mu_1} \langle \mu_1|[[H_0,\tau_{\gamma_1}],\tau_{\nu_1}] + [[[H_0,\tau_{\gamma_1}],\tau_{\nu_1}],X]|HF\rangle \\ + \sum_{\mu_2} \bar{t}^{(0)}_{\mu_2} \langle \mu_2|[[H_0,\tau_{\gamma_1}],\tau_{\nu_1}] + [[[H_0,\tau_{\gamma_1}],\tau_{\nu_1}],X] \\ + [[[[H,\tau_{\gamma_1}],\tau_{\nu_1}],X],X]|HF\rangle \end{pmatrix} \quad \begin{pmatrix} \langle HF|[[H_0,\tau_{\gamma_1}],\tau_{\nu_2}] + [[[H_0,\tau_{\gamma_1}],\tau_{\nu_2}],X]|HF\rangle \\ + \sum_{\mu_1} \bar{t}^{(0)}_{\mu_1} \langle \mu_1|[[H_0,\tau_{\gamma_1}],\tau_{\nu_2}] + [[[H_0,\tau_{\gamma_1}],\tau_{\nu_2}],X]|HF\rangle \\ + \sum_{\mu_2} \bar{t}^{(0)}_{\mu_2} \langle \mu_2|[[H_0,\tau_{\gamma_1}],\tau_{\nu_2}] + [[[H_0,\tau_{\gamma_1}],\tau_{\nu_2}],X]|HF\rangle \end{pmatrix}$$

$$\begin{pmatrix} \langle HF|[[H_0,\tau_{\gamma_2}],\tau_{\nu_1}] + [[[H_0,\tau_{\gamma_2}],\tau_{\nu_1}],X]|HF\rangle \\ + \sum_{\mu_1} \bar{t}^{(0)}_{\mu_1} \langle \mu_1|[[H_0,\tau_{\gamma_2}],\tau_{\nu_1}] + [[[H_0,\tau_{\gamma_2}],\tau_{\nu_1}],X]|HF\rangle \\ + \sum_{\mu_2} \bar{t}^{(0)}_{\mu_2} \langle \mu_2|[[H_0,\tau_{\gamma_2}],\tau_{\nu_1}] + [[[H_0,\tau_{\gamma_2}],\tau_{\nu_1}],X]|HF\rangle \end{pmatrix} \quad \begin{pmatrix} \langle HF|[[H_0,\tau_{\gamma_2}],\tau_{\nu_2}] + [[[H_0,\tau_{\gamma_2}],\tau_{\nu_2}],X]|HF\rangle \\ + \sum_{\mu_1} \bar{t}^{(0)}_{\mu_1} \langle \mu_1|[[H_0,\tau_{\gamma_2}],\tau_{\nu_2}] + [[[H_0,\tau_{\gamma_2}],\tau_{\nu_2}],X]|HF\rangle \\ + \sum_{\mu_2} \bar{t}^{(0)}_{\mu_2} \langle \mu_2|[[H_0,\tau_{\gamma_2}],\tau_{\nu_2}] + [[[H_0,\tau_{\gamma_2}],\tau_{\nu_2}],X]|HF\rangle \end{pmatrix}$$

Now using that the CC operator, X, for a system with N electrons can be written as

$$X = X_1 + X_2 + \cdots + X_N \tag{3.6}$$

and the fact that the $\boldsymbol{\mathcal{F}}^{CCSD}$ matrix can be simplified even more using the X_1 transformed Hamiltonian, $\hat{H}$

$$\hat{H} = \exp(-X_1) H \exp(X_1) \tag{3.7}$$

the $\boldsymbol{\mathcal{F}}^{CCSD}$ matrix takes the form

$$\boldsymbol{\mathcal{F}}^{CCSD} = \begin{pmatrix} \langle HF|[[H_0,\tau_{\gamma_1}],\tau_{\nu_1}]HF\rangle & \\ +\sum_{\mu_1} \bar{t}^{(0)}_{\mu_1}\langle\mu_1|[[\hat{H}_0,\tau_{\gamma_1}],\tau_{\nu_1}]|HF\rangle & \sum_{\mu_1} \bar{t}^{(0)}_{\mu_1}\langle\mu_1|[[\hat{H}_0,\tau_{\gamma_1}],\tau_{\nu_2}]|HF\rangle \\ \quad +\sum_{\mu_2} \bar{t}^{(0)}_{\mu_2}\langle\mu_2|\Big([[\hat{H}_0,\tau_{\gamma_1}],\tau_{\nu_1}] & +\sum_{\mu_2} \bar{t}^{(0)}_{\mu_2}\langle\mu_2|[[\hat{H}_0,\tau_{\gamma_1}],\tau_{\nu_2}]|HF\rangle \\ \quad +[[[H_0,\tau_{\gamma_1}],\tau_{\nu_1}],X^{(0)}_2]\Big)|HF\rangle & \\ & \\ \sum_{\mu_1} \bar{t}^{(0)}_{\mu_1}\langle\mu_1|[[\hat{H}_0,\tau_{\gamma_2}],\tau_{\nu_1}]|HF\rangle & \sum_{\mu_2} \bar{t}^{(0)}_{\mu_2}\langle\mu_2|[[H_0,\tau_{\gamma_2}],\tau_{\nu_2}]|HF\rangle \\ +\sum_{\mu_2} \bar{t}^{(0)}_{\mu_2}\langle\mu_2|[[\hat{H}_0,\tau_{\gamma_2}],\tau_{\nu_1}]|HF\rangle & \end{pmatrix}$$

Splitting the second order excitations into S and T gives a three dimensional matrix, which has some extra terms compared to the one used in the ECC2 model.

$$
\boldsymbol{\mathcal{F}}^{CCSD} = \begin{pmatrix}
\begin{array}{c}
\langle HF|[[\hat{H}_0,\tau_{\gamma_1}],\tau_{\nu_1}]HF\rangle \\
+\sum_{\mu_1}\bar{t}^{(0)}_{\mu_1}\langle\mu_1|[[\hat{H}_0,\tau_{\gamma_1}],\tau_{\nu_1}]|HF\rangle \\
+\sum_{\mu_2^T}\bar{t}^{(0)}_{\mu_2^T}\langle\mu_2^T|\Big([[\hat{H}_0,\tau_{\gamma_1}],\tau_{\nu_1}] \\
+[[[H_0,\tau_{\gamma_1}],\tau_{\nu_1}],X_2^{(0)}]\Big)|HF\rangle \\
+\sum_{\mu_2^S}\bar{t}^{(0)}_{\mu_2^S}\langle\mu_2^S|\Big([[\hat{H}_0,\tau_{\gamma_1}],\tau_{\nu_1}] \\
+[[[H_0,\tau_{\gamma_1}],\tau_{\nu_1}],X_2^{(0)}]\Big)|HF\rangle
\end{array} &
\begin{array}{c}
\sum_{\mu_1}\bar{t}^{(0)}_{\mu_1}\langle\mu_1|[[\hat{H}_0,\tau_{\gamma_1}],\tau_{\nu_2^T}]|HF\rangle \\
+\sum_{\mu_2^T}\bar{t}^{(0)}_{\mu_2^T}\langle\mu_2^T|[[\hat{H}_0,\tau_{\gamma_1}],\tau_{\nu_2^T}]|HF\rangle \\
+\sum_{\mu_2^S}\bar{t}^{(0)}_{\mu_2^S}\langle\mu_2^S|[[\hat{H}_0,\tau_{\gamma_1}],\tau_{\nu_2^T}]|HF\rangle
\end{array} &
\begin{array}{c}
\sum_{\mu_1}\bar{t}^{(0)}_{\mu_1}\langle\mu_1|[[\hat{H}_0,\tau_{\gamma_1}],\tau_{\nu_2^S}]|HF\rangle \\
+\sum_{\mu_2^T}\bar{t}^{(0)}_{\mu_2^T}\langle\mu_2^T|[[\hat{H}_0,\tau_{\gamma_1}],\tau_{\nu_2^S}]|HF\rangle \\
+\sum_{\mu_2^S}\bar{t}^{(0)}_{\mu_2^S}\langle\mu_2^S|[[\hat{H}_0,\tau_{\gamma_1}],\tau_{\nu_2^S}]|HF\rangle
\end{array} \\
\begin{array}{c}
\sum_{\mu_1}\bar{t}^{(0)}_{\mu_1}\langle\mu_1|[[\hat{H}_0,\tau_{\gamma_2^T}],\tau_{\nu_1}]|HF\rangle \\
+\sum_{\mu_2^T}\bar{t}^{(0)}_{\mu_2^T}\langle\mu_2^T|[[\hat{H}_0,\tau_{\gamma_2^T}],\tau_{\nu_1}]|HF\rangle \\
+\sum_{\mu_2^S}\bar{t}^{(0)}_{\mu_2^S}\langle\mu_2^S|[[\hat{H}_0,\tau_{\gamma_2^T}],\tau_{\nu_1}]|HF\rangle
\end{array} &
\begin{array}{c}
\sum_{\mu_2^T}\bar{t}^{(0)}_{\mu_2^T}\langle\mu_2^T|[[\hat{H}_0,\tau_{\gamma_2^T}],\tau_{\nu_2^T}]|HF\rangle \\
+\sum_{\mu_2^S}\bar{t}^{(0)}_{\mu_2^S}\langle\mu_2^S|[[\hat{H}_0,\tau_{\gamma_2^T}],\tau_{\nu_2^T}]|HF\rangle
\end{array} &
\begin{array}{c}
\sum_{\mu_2^T}\bar{t}^{(0)}_{\mu_2^T}\langle\mu_2^T|[[\hat{H}_0,\tau_{\gamma_2^T}],\tau_{\nu_2^S}]|HF\rangle \\
+\sum_{\mu_2^S}\bar{t}^{(0)}_{\mu_2^S}\langle\mu_2^S|[[\hat{H}_0,\tau_{\gamma_2^T}],\tau_{\nu_2^S}]|HF\rangle
\end{array} \\
\begin{array}{c}
\sum_{\mu_1}\bar{t}^{(0)}_{\mu_1}\langle\mu_1|[[\hat{H}_0,\tau_{\gamma_2^S}],\tau_{\nu_1}]|HF\rangle \\
+\sum_{\mu_2^T}\bar{t}^{(0)}_{\mu_2^T}\langle\mu_2^T|[[\hat{H}_0,\tau_{\gamma_2^S}],\tau_{\nu_1}]|HF\rangle \\
+\sum_{\mu_2^S}\bar{t}^{(0)}_{\mu_2^S}\langle\mu_2^S|[[\hat{H}_0,\tau_{\gamma_2^S}],\tau_{\nu_1}]|HF\rangle
\end{array} &
\begin{array}{c}
\sum_{\mu_2^T}\bar{t}^{(0)}_{\mu_2^T}\langle\mu_2^T|[[\hat{H}_0,\tau_{\gamma_2^S}],\tau_{\nu_2^T}]|HF\rangle \\
+\sum_{\mu_2^S}\bar{t}^{(0)}_{\mu_2^S}\langle\mu_2^S|[[\hat{H}_0,\tau_{\gamma_2^S}],\tau_{\nu_2^T}]|HF\rangle
\end{array} &
\begin{array}{c}
\sum_{\mu_2^T}\bar{t}^{(0)}_{\mu_2^T}\langle\mu_2^T|[[\hat{H}_0,\tau_{\gamma_2^S}],\tau_{\nu_2^S}]|HF\rangle \\
+\sum_{\mu_2^S}\bar{t}^{(0)}_{\mu_2^S}\langle\mu_2^S|[[\hat{H}_0,\tau_{\gamma_2^S}],\tau_{\nu_2^S}]|HF\rangle
\end{array}
\end{pmatrix}
$$

It is possible to obtain the ECC2 $\boldsymbol{\mathcal{F}}$ matrix from the CCSD $\boldsymbol{\mathcal{F}}^{CCSD}$ matrix, and to compute the $\boldsymbol{\mathcal{F}}$ matrix in the most cost efficient way, the goal is to use as few calls as possible. Even though using the $\boldsymbol{\mathcal{F}}^{CC2}$ is cheaper, we will need more calls compared to using only $\boldsymbol{\mathcal{F}}^{CCSD}$. Comparing it to the ECC2 $\boldsymbol{\mathcal{F}}$ matrix we see that the upper left terms are equal except for the $\langle \mu_2^S|$ part where we need to subtract the zero order $S_2^{(0)}$ amplitudes. The lower right triangular matrix including the diagonal is also almost equal for ECC2 and CCSD except for the $\langle \mu_2^S$ terms. The remaining terms are identical for EEC2 and CCSD. Subtraction gives a picture of what terms in the $\boldsymbol{\mathcal{F}}^{CCSD}$ matrix that do not appear in the ECC2 $\boldsymbol{\mathcal{F}}$ matrix.

$$\boldsymbol{\mathcal{F}}^{CCSD} - \boldsymbol{\mathcal{F}} = \tag{3.8}$$

$$\begin{pmatrix} \sum_{\mu_2^S} \bar{t}^{(0)}_{\mu_2^S} \langle \mu_2^S | [[[\hat{H}_0, \tau_{\gamma 1}], \tau_{\nu_1}], S_2^{(0)}] | HF \rangle & 0 & \sum_{\mu_2^S} \bar{t}^{(0)}_{\mu_2^S} \langle \mu_2^S | [[\hat{H}_0, \tau_{\gamma_1}], \tau_{\nu_2^S}] | HF \rangle \\ 0 & \sum_{\mu_2^S} \bar{t}^{(0)}_{\mu_2^S} \langle \mu_2^S | [[\hat{H}_0, \tau_{\gamma_2^T}], \tau_{\nu_2^T}] | HF \rangle & \sum_{\mu_2^S} \bar{t}^{(0)}_{\mu_2^S} \langle \mu_2^S | [[\hat{H}_0, \tau_{\gamma_2^T}], \tau_{\nu_2^S}] | HF \rangle \\ \sum_{\mu_2^S} \bar{t}^{(0)}_{\mu_2^S} \langle \mu_2^S | [[\hat{H}_0, \tau_{\gamma_2^S}], \tau_{\nu_1}] | HF \rangle & \sum_{\mu_2^S} \bar{t}^{(0)}_{\mu_2^S} \langle \mu_2^S | [[\hat{H}_0, \tau_{\gamma_2^S}], \tau_{\nu_2^T}] | HF \rangle & \sum_{\mu_2^S} \bar{t}^{(0)}_{\mu_2^S} \langle \mu_2^S | [[\hat{H}_0, \tau_{\gamma_2^S}], \tau_{\nu_2^S}] | HF \rangle \end{pmatrix}$$

The routine that computes the $\boldsymbol{\mathcal{F}}$ matrix therefore has to be called several times and the the following system, where i represents the number of times the routine is called, can be used.

$$\sum_i \boldsymbol{t}_i^{(A)}(-\omega)\boldsymbol{\mathcal{F}}_i^{CCSD}{}_i\boldsymbol{R} = \boldsymbol{t}^{(A)}(-\omega)\boldsymbol{\mathcal{F}}\boldsymbol{R} \tag{3.9}$$

where the routine can be manipulated by setting parts of the multipliers, $\bar{\boldsymbol{t}}^{(0)}$, the vectors, $\boldsymbol{t}^{(A)}(-\omega)$ and $\boldsymbol{R}$ or the zero order amplitude vector $\boldsymbol{X}^{(0)}$ to zero. Each of these vectors include a single excitation part, a CCSD part, T, and a CC2 part, S, as shown for the first order multipliers in Eq. (2.37). The minimum number of steps to obtain the ECC2 $\boldsymbol{\mathcal{F}}$ matrix is four. By first setting the $\bar{t}^{(0)}_{\mu_2^S}$ to zero we get the ground state, single excitation and the T-part of the double excitations. The second time the routine is called, the S-part of $\boldsymbol{t}^{(A)}(-\omega)$ and $\boldsymbol{R}$ as well as $\bar{t}^{(0)}_{\mu_1}$ and $\bar{t}^{(0)}_{\mu_2^T}$ are set to zero. This gives the right S-terms to $\mathcal{F}_{\gamma_1\nu_1}$, $\mathcal{F}_{\gamma_1\nu_2^T}$ and $\mathcal{F}_{\gamma_2^T\nu_1}$ but we now have two extra terms that need to be subtracted from the matrix. First setting $\bar{t}^0$ and the zero order amplitude vector in the same way as in the previous call, and choosing only the T-part of $\boldsymbol{t}^{(A)}(-\omega)$ and $\boldsymbol{R}$ we can subtract the extra $\langle\mu_2^S|$-term in $\mathcal{F}_{\gamma_2^T\nu_2^T}$. For the fourth and final call $\bar{t}^{(0)}$ will be set to zero as well as the T- and S-parts of $\boldsymbol{t}^{(A)}(-\omega)$, $\boldsymbol{R}$ and the zero order amplitude vector. Now the extra ground state term in $\mathcal{F}_{\gamma_1\nu_1}$ can be subtracted. However, because the terms containing the $\boldsymbol{\mathcal{F}}$ matrix have to be calculated for all the excitations, the computational cost can be reduced by using an auxiliary vector $\boldsymbol{Y}$ when calculating the transition moments.

$$\boldsymbol{Y} = \boldsymbol{\mathcal{F}}\boldsymbol{R} \tag{3.10}$$

As the row vectors of $\boldsymbol{\mathcal{F}}$ are dotted with the right eigenvectors we obtain $\boldsymbol{Y}$, and the Eq. (3.11) is solved. The response equation can now be simplified as shown in Eq. (3.12) and (3.13).

$$\bar{\boldsymbol{M}} = \boldsymbol{Y}(\omega_k\boldsymbol{1} + \boldsymbol{A})^{-1} \tag{3.11}$$

$$\lim_{\omega\to\omega_k}(\omega-\omega_k)\langle\langle A,B\rangle\rangle_\omega = \tag{3.12}$$
$$\frac{1}{2}\left[\left(C_\nu^{(A)}R_{\nu k}-\sum_\gamma t_\gamma^{(A)}\bar{M}_{\gamma k}\right)\xi_k^{(B)}-\left(\left(C_\nu^{(B)}R_{\nu k}+\sum_\gamma t_\gamma^{(B)}\bar{M}_{\gamma k}\right)\xi_k^{(A)}\right)^*\right]$$

$$\lim_{\omega\to-\omega_k}(\omega+\omega_k)\langle\langle A,B\rangle\rangle_\omega = \tag{3.13}$$
$$\frac{1}{2}\left[\left(-C_\nu^{(B)}R_{\nu k}+\sum_\gamma t_\gamma^{(B)}\bar{M}_{\gamma k}\right)\xi_k^{(A)}+\left(\left(C_k^{(A)}R_{\nu k}+\sum_\gamma t_\gamma^{(A)}\bar{M}_{\gamma k}\right)\xi_k^{(B)}\right)^*\right]$$

When using Eq. (3.12) and (3.13), the $\boldsymbol{\mathcal{F}}$-terms cannot be computed as described earlier. That is because we no longer have the flexibility of manipulating two vectors to obtain the ECC2 $\boldsymbol{\mathcal{F}}$ matrix. We now only have one vector to get the auxiliary vector $\boldsymbol{Y}$ that i used to calculate the $\boldsymbol{\mathcal{F}}$-term. The system that needs to be solved can now be viewed as

$$\boldsymbol{Y}=\sum_i \boldsymbol{\mathcal{F}}_i^{T\,i}\boldsymbol{R}+\sum_j \boldsymbol{\mathcal{F}}_j^{S\,j}\boldsymbol{R} \tag{3.14}$$

It is, however, most convenient to only use the CCSD model, i.e. $\boldsymbol{\mathcal{F}}^T$ and we can get the whole $\boldsymbol{Y}$ vector computed calling the routine only four times.

1. First setting only $\bar{t}_{\mu_2^S}^{(0)}$ to zero, we get the biggest part of the $\boldsymbol{Y}$ vector.

$$
{}^1\boldsymbol{Y} = \begin{pmatrix}
\big\{\langle HF|[[H_0,\tau_{\gamma_1}],\tau_{\nu_1}]|HF\rangle \\
+\sum_{\mu_2^T}\bar{t}^{(0)}_{\mu_2^T}\langle\mu_2^T|[[\hat{H}_0,\tau_{\gamma_1}],\tau_{\nu_1}]+[[[\hat{H}_0,\tau_{\gamma_1}],\tau_{\nu_1}],X_2^{(0)}]|HF\rangle\big\}R_1 \\
+\big\{\sum_{\mu_1}\bar{t}^{(0)}_{\mu_1}\langle\mu_1|[[\hat{H}_0,\tau_{\gamma_1}],\tau_{\nu_2^T}]|HF\rangle+\sum_{\mu_2^T}\bar{t}^{(0)}_{\mu_2^T}\langle\mu_2^T|[[\hat{H}_0,\tau_{\gamma_1}],\tau_{\nu_2^T}]|HF\rangle\big\}R_{T_2} \\
+\big\{\sum_{\mu_1}\bar{t}^{(0)}_{\mu_1}\langle\mu_1|[[\hat{H}_0,\tau_{\gamma_1}],\tau_{\nu_2^S}]|HF\rangle+\sum_{\mu_2^T}\bar{t}^{(0)}_{\mu_2^T}\langle\mu_2^T|[[\hat{H}_0,\tau_{\gamma_1}],\tau_{\nu_2^S}]|HF\rangle\big\}R_{S_2} \\
\\
\big\{\sum_{\mu_1}\bar{t}^{(0)}_{\mu_1}\langle\mu_1|[[\hat{H}_0,\tau_{\gamma_2^T}],\tau_{\nu_1}]|HF\rangle+\sum_{\mu_2^T}\bar{t}^{(0)}_{\mu_2^T}\langle\mu_2^T|[[\hat{H}_0,\tau_{\gamma_2^T}],\tau_{\nu_1}]|HF\rangle\big\}R_1 \\
+\sum_{\mu_2^T}\bar{t}^{(0)}_{\mu_2^T}\langle\mu_2^T|[[\hat{H}_0,\tau_{\gamma_2^T}],\tau_{\nu_2^T}]|HF\rangle R_{T_2} \\
+\sum_{\mu_2^T}\bar{t}^{(0)}_{\mu_2^T}\langle\mu_2^T|[[\hat{H}_0,\tau_{\gamma_2^T}],\tau_{\nu_2^S}]|HF\rangle R_{S_2} \\
\\
\big\{\sum_{\mu_1}\bar{t}^{(0)}_{\mu_1}\langle\mu_1|[[\hat{H}_0,\tau_{\gamma_2^S}],\tau_{\nu_1}]|HF\rangle+\sum_{\mu_2^T}\bar{t}^{(0)}_{\mu_2^T}\langle\mu_2^T|[[\hat{H}_0,\tau_{\gamma_2^S}],\tau_{\nu_1}]|HF\rangle\big\}R_1 \\
+\sum_{\mu_2^T}\bar{t}^{(0)}_{\mu_2^T}\langle\mu_2^T|[[\hat{H}_0,\tau_{\gamma_2^S}],\tau_{\nu_2^T}]|HF\rangle R_{T_2} \\
+\sum_{\mu_2^T}\bar{t}^{(0)}_{\mu_2^T}\langle\mu_2^T|[[\hat{H}_0,\tau_{\gamma_2^S}],\tau_{\nu_2^S}]|HF\rangle R_{S_2}
\end{pmatrix}
$$

2. Secondly $R_1^{(A)}$, $R_{S_2}^{(A)}$, $\bar{t}^{(0)}_{\mu_1}$ and $\bar{t}^{(0)}_{\mu_2^T}$ are all set to zero. After calling the routine the first time, ${}^2Y_{T_2}$ and ${}^2Y_{S_2}$ are reset to zero. Thus ending up with

$$
{}^2\boldsymbol{Y} = \begin{pmatrix}
\sum_{\mu_2^S}\bar{t}^{(0)}_{\mu_2^S}\langle\mu_2^S|[[\hat{H}_0,\tau_{\gamma_1}],\tau_{\nu_2^T}]|HF\rangle R_{T_2} \\
\\
0 \\
\\
0
\end{pmatrix}
$$

3. Similarly, for the third call $R_{T_2}^{(A)}$, $R_{S_2}^{(A)}$, $\bar{t}^{(0)}_{\mu_1}$, $\bar{t}^{(0)}_{\mu_2^T}$ and the S part of the zero order amplitude are set to zero, and again after the routine is called ${}^2Y_{S_2}$ is reset to zero, giving

$$
{}^{3}\boldsymbol{Y} = \begin{pmatrix} \big\{\langle HF|[[H_0,\tau_{\gamma_1}],\tau_{\nu_1}]|HF\rangle \\ +\sum_{\mu_2^S} \bar{t}^{(0)}_{\mu_2^S}\langle \mu_2^S|[[\hat{H}_0,\tau_{\gamma_1}],\tau_{\nu_1}] + [[[\hat{H}_0,\tau_{\gamma_1}],\tau_{\nu_1}],T_2^{(0)}]|HF\rangle\big\}R_1 \\ \\ \sum_{\mu_2^S} \bar{t}^{(0)}_{\mu_2^S}\langle \mu_2^S|[[\hat{H}_0,\tau_{\gamma_2^T}],\tau_{\nu_1}]|HF\rangle R_1 \\ \\ 0 \end{pmatrix}
$$

4. The fourth time the routine is called we set the whole $\bar{\boldsymbol{t}}^{(0)}$ vector to zero as well as $R^{(A)}_{\mu_2^T}$ and $R^{(A)}_{\mu_2^S}$. This term needs to be subtracted from the rest and we choose a negative sign, resulting in

$$
{}^{4}\boldsymbol{Y} = -\begin{pmatrix} \langle HF|[[H_0,\tau_{\gamma_1}],\tau_{\nu_1}]|HF\rangle R_1 \\ 0 \\ 0 \end{pmatrix}
$$

Eq. (3.14) will now give us the ECC2 $\boldsymbol{\mathcal{F}R}$ term using ${}^{i}\boldsymbol{Y}$ as described above. Using the $\boldsymbol{Y}^{(A)}$ vector (Method 2) should reduce the computational cost compared to using Eq. (2.50) and (2.51) (Method 1). This is because using Method 2, $\boldsymbol{Y}^{(A)}$ only needs to be calculated once for each eigenvector $\langle k|$, while for Method 1 each term is computed $m \times n$ times. Chosing Method 2 instead of method one should therefore result in a m-fold reduction in computational cost.

4 Testing

As discussed in the previous section, this work has been focused on deriving the ECC2 expressions needed for the transition moment and development and implementation of the calculation of the $\boldsymbol{\mathcal{F}}$ matrix that affects the transition moment. The test results are an indication of the present state of the pilot code. Two different systems were chosen for the testing.

4.1 Initial Testing

To run the first tests, a small system was chosen; one single water molecule. Figure 4 shows how oxygen was treated as the active space, while both hydrogens were treated with CC2. The molecule was built in Avogadro [45] and the cc-pVDZ basis set was used. The initial testing gave results that were in thread with what was excpect, i.e. somewhere between the CC2 and the CCSD results. They are, however, not presented here as they are not the correct ECC2 transition moments. The results give only an indication of the model, and even though the values are closer to CCSD than CC2 as expected, this still does not prove that the current version of the code is correct. Further testing is therefore necessary to validate the pilot code and obtain verified ECC2 transition moments.

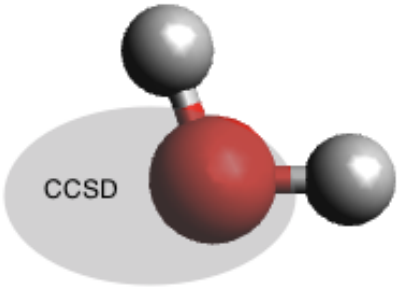

Figure 4: H_2O

4.2 Indepth Testing

To further investigate the model, a slightly bigger system was chosen; one water molecule and one Helium atom. Figures 5 and 6 show the system using two different active spaces. The particles are separated by 100 Å, and because of the large distance between them, an excitation in the active space should give the same result as CCSD while an excitation in the inactive space should give CC2 results. In Figure 5 the whole water molecule is the active space and this system is refered to as ECC2A, while Figure 6 shows the He atom as the active space and is refered to as ECC2B. The Pople type basis set 6-31G was used for the calculations.

Figure 5: ECC2A

Figure 6: ECC2B

The ECC2A model reproduces CCSD results, while the ECC2B model values deviate from the CC2 results. The ECC2A and ECC2B test runs suggest that the lowest excitations all occur within the water molecule. This is because the ECC2A model gives the same results as CCSD. When the active space is changed to the helium atom, the outcome is closer to CC2 results. By inspecting the different $\boldsymbol{Y}$ vectors it is possible to unveil why the two ECC2 models give different results. In fact, a test where the ECC2A model was used and only the ${}^{1}\boldsymbol{Y}$ was calculated

gave the same result as when all four $\boldsymbol{Y}$ vectors were added together. Because the S-part of both the eigenvectors, the multipliers and the zero order amplitude was zero for these four excitations, the ${}^{1}\boldsymbol{Y}$ vector was simply the same as calculating the regular CCSD $\boldsymbol{Y}$ vector, while the addition from ${}^{3}\boldsymbol{Y}$ was again subtracted using ${}^{4}\boldsymbol{Y}$. The ECC2B model, however, requires modification of the eigenvectors, multipliers, and all except ${}^{2}\boldsymbol{Y}$ contribute to the final result, in contrast to the ECC2A model. It appears that the modification of the vectors affects the result, but a solution to this bug has not yet been found.

The left and right transition matrix elements can be investigated to narrow down the root of the problem. Eq. (2.56) and (2.55) show the components of the right and left transition matrix element respectively. It can be found by inspection that the ECC2B right transition matrix elements deviate from the CC2 values. As Eq. (2.56) shows this is the term including the $\boldsymbol{\mathcal{F}}$ matrix. The right transition matrix element also includes the right eigenvectors and the $\boldsymbol{C}^{(O)}$ vector. Finally, printing and comparing the $\boldsymbol{Y}$ vectors for ECC2B and CC2 shos that they indeed differ and the current version of the code therefore needs to be further investigated and debugged.

5 Conclusion

The theory and implementation plan presented here suggest that the ECC2 model should give transition moments that are related to CCSD and CC2 in the same way excitation energies have been proven to be. The current version of the code, however, does not fulfill these expectations as the results suggest, presumably due to a bug. Because the implementation is still under developement, the expected reduction in computational complexity cannot be investigated and for the time being, the ECC2 model actually requires more time than equivalent CCSD calculations.

6 Future Work

As the current version of the code that computes the ECC2 transition moment does not give the expected values, it needs to be further investigated and tested. Dividing the system into two levels is the simplest form of a multi level coupled cluster model, and because the work presented here has not given successful results, the addition of a third level has not been tested, even though it should be possible with the current version of the code. When the bilevel version has been proven successful, the model can be expanded to include more levels.

Versions of the ECC2 model, where a third level has been added, have been tested for excitation energies and also that part of the model is still under developement. Because the the pilot version of the code does not allow for any savings in computational cost, it is not appropriate to run calculations on larger systems yet. Developing a more efficient version of the code is therefore a current objective.

Bibliography

[1] S. Karin, N. P. Smith, and J. F. Hawley. The supercomputer era. *Am. Inst. Phys.*, 1988.

[2] D. A. Joiner, R. M. Panoff, P. Gray, T. Murphy, and C. Peck. Supercomputer based laboratories and the evolution of the personal computer based laboratory. *Am. J. Phys.*, 2008.

[3] *Molecular electronic-structure theory.* John Wiley and Sons Ltd, 2000.

[4] J. Kongsted, A. Osted, and K. V. Mikkelsen. Linear response functions for coupled cluster/molecular mechanics including polarization interactions. *J. Chem. Phys.*, 2002.

[5] A. Osted, J. Kongsted, K. V. Mikkelsen, and O. Christiansen. Linear response properties of liquid water calculated using CC2 and CCSD within different molecular mechanics methods. *J. Phys. Chem.*, 2004.

[6] S. D. Wetmore, R. J. Boyd, L. A. Eriksson, and A. Laaksonen. A combined quantum mechanics and molecular dynamics study of small Jahn-Teller distorted hydrocarbons: Another difficult test for density functional theory. *J. Chem. Phys.*, 1999.

[7] Z. Cai, K. Sendt, and J. R. Reimers. Failure of density functional theory and time dependent density functional theory for large extended π systems. *J. Chem. Phys.*, 2002.

[8] M. J. Paterson, O. Christiansen, F. Pawlowski, P. Jørgensen, C. Hättig, T. Helgaker, and P. Salek. Benchmarking two-photon absorption with CC3 quadratic response theory, and comparison with density-functional response theory. *J. Chem. Phys.*, 2006.

[9] R. H. Myhre, A. Sánchez de Merás, and H. Koch. The extended cc2 model ecc2. *J. Mol. Phys.*, 2013.

[10] O. Christiansen, H. Koch, and P. Jørgensen. The second-order approximate coupled cluster singles and doubles model CC2. *Chem. Phys. Let. 243*, 1995.

[11] J. Olsen, P. Jørgensen, H. Koch, A. Balkova, and R. J. Bartlett. Full configuration-interaction and state of the art correlation calculations on water in a valence doublezeta basis with polarization functions. *J. Chem. Phys.*, 1996.

[12] A. Sánchez de Merás, H. Koch, I. G. Cuesta, and L. Boman. Cholesky decomposition-based definition of atomic subsystems in electronic structure calculations. *J. Chem. Phys.*, 2010.

[13] T. B. Pedersen, A. Sánchez de Merás, and H. Koch. Polarizability and optical rotation calculated from the approximate coupled cluster singles and doubles CC2 linear response theory using Cholesky decompositions. *J. Chem. Phys.*, 2004.

[14] J. L. Cacheiro, T. B. Pedersen, B. Fernández, A. Sánchez de Merás, and H. Koch. The ccsd(t) model with cholesky decomposition of orbital energy denominators. *Int. J. Quantum Chem.*, 2010.

[15] P. Baudin, J. Sánchez Marín, I. G. Cuesta, and A. Sánchez de Merás. Calculation of excitation energies from the CC2 linear response theory using Cholesky decomposition. *J. Chem. Phys.*, 2014.

[16] *Molecular Quantum Mechanics*. Oxford University Press, 2011.

[17] T.B. Pedersen. Introduction to response theory. *Handb. Comp. Chem.*, 2012.

[18] *Physical Chemistry*. Oxford University Press, 2010.

[19] N. J. Turro. *Modern molecular Photochemistry*. University Science Books, 1991.

[20] J. Olsen and P. Jørgensen. Linear and nonlinear response functions for an exact and for an MCSCF state. *J. Chem. Phys.*, 1985.

[21] *Modern Quantum Chemistry: Introduction to Advanced Electronic Structure Theory*. Dover Publications, Inc., 1989.

[22] H. J. Monkhorst. Calculation of properties with the coupled cluster method. *Int. J. Quantum Chem.*, 1977.

[23] R. J. Bartlett. Coupled-cluster approach to molecular structure and spectra: A step toward predictive quantum chemistry. *J. Phys. Chem.*, 1989.

[24] O. Christiansen, H. Koch, and P. Jørgensen. Response functions in the cc3 iterative triple excitation model. *J. Chem. Phys.*, 1995.

[25] H. Larsen, J. Olsen, C. Hättig, P. Jørgensen, O. Christiansen, and J. Gauss. Polarizabilities and first hyperpolarizabilities of hf, ne and bh from full configuration interaction and coupled cluster calculations. *J. Chem. Phys.*, 1999.

[26] S. A. Kucharski and R. J. Bartlett. The coupled-cluster single, double, triple and quadruple excitation method. *J. Chem. Phys.*, 1992.

[27] L. Thøgersen. *Optimization of densities in Hartree-Fock and density-functional theory atomic orbital based response theory and benchmarking for radicals.* PhD thesis, Univerity of Aarhus, 2005.

[28] K. Raghavachari and G. W. Trucks. A fifth-order perturbation comparison of electron correlation theories. *Chem. Phys. Let. 157*, 1989.

[29] J. Řezáč and P. Hobza. Describing noncovalent interactions beyond the common approximations: How accurate is the "gold standard", ccsd(t) at the complete basis set limit? *J. Chem. Theory Compute.2013.*

[30] F. Aquilante, T. B. Pedersen, A. Sánchez de Merás, and H. Koch. Fast noniterative orbital localization for large molecules. *J. Chem. Phys.*, 2006.

[31] C. Ochsenfeld, J. Kussmann, and D. S. Lambrecht. Linear-scaling methods in quantum chemistry. *Rev. Comp. Chem.*, 2007.

[32] H. Koch, A. Sánchez de Merás, and T. B. Pedersen. Reduced scaling in electronic structure calculations using Cholesky decompositions. *J. Chem. Phys.*, 2003.

[33] A. Sánchez de Merás. Decanal. Universitat de València.

[34] H. Koch and A. Sánchez de Merás. Size-intensitive decomposition of orbital energy denominators. *J. Chem. Phys.*, 2000.

[35] *Linear-scaling techniques in computational chemistry and physics*. Springer, 2011.

[36] E. Dalgaard and H. J. Monkhorst. Some aspects of the time-dependent coupled cluster approach to dynamic response functions. *Phys. Rev. A*, 1983.

[37] H. Sekino and R. J. Bartlett. A linear response coupled cluster theory for excitation energy. *Int. J. Quantum Chem.*, 1984.

[38] H. Koch and P. Jørgensen. Coupled cluster response functions. *J. Chem. Phys.*, 1990.

[39] T. B. Pedersen and H. Koch. Coupled cluster response functions revisited. *J. Chem. Phys.*, 1997.

[40] H. Koch, R.Kobayashi, A. Sánchez de Merás, and P. Jørgensen. Calculation of sizeintensitive transition moments from the coupled cluster singles and doubles linear response function. *J. Chem. Phys.*, 1994.

[41] K. Sasagane, F. Aiga, and R. Itoh. Higher-order response theory based on the quasienergy derivatives: The derivation of the frequancy-dependent polarizabilties and hyperpolarizabilities. *J. Chem. Phys.*, 1993.

[42] R. H. Myhre. Development and implementation of extended cc2 models. Master's thesis, NTNU, 2013.

[43] Ove Christiansen, Poul Jørgensen, and Christof Hättig. Response functions from fourier component variational perturbation theory applied to a time-averaged quasienergy. *Int. J. Quantum Chem.*, 1997.

[44] K. Aidas, C. Angeli, K. L. Bak, V. Bakken, R. Bast, L. Boman, O. Christiansen, R. Cimiraglia, S. Coriani, P. Dahle, E. K. Dalskov, U. Ekström, T. Enevoldsen, J. J. Eriksen, P. Ettenhuber, B. Fernández, L. Ferrighi, H. Fliegl, L. Frediani, K. Hald, A. Halkier, C. Hättig, H. Heiberg, T. Helgaker, A. C. Hennum, H. Hettema, E. Hjertenæs, S. Høst, I.-M. Høyvik, M. F.

Iozzi, B. Jansik nad H. J. Aa. Jensen, D. Jonsson, P. Jørgensen, J. Kauczor, S. Kirpekar, T. Kjærgaard, W. Klopper, S. Knecht, R. Kobayashi, H. Koch, J. Kongsted, A. Krapp, K. Kristensen, A. Ligabue, O. B. Lutnæs, J. I. Melo, K. V. Mikkelsen, R. H. Myhre, C. Neiss, C. B. Nielsen, P. Norman, J. Olsen, J. M. H. Olsen, A. Osted, M. J. Packer, F. Pawlowski, T. B. Pedersen, P. F. Provasi, S. Reine, Z. Rinkevicius, T. A. Ruden, K. Ruud, V. Rybkin, P. Salek, C. C. M. Samson, A. Sánchez de Merás, T. Saue, S. P. A. Sauer, B. Schimmelpfennig, K. Sneskov, A. H. Steindal, K. O. Sylvester-Hvid, P. R. Taylor, A. M. Teale, E. I. Tellgren, D. P. Tew, A. J. Thorvaldsen, L. Thøgersen, O. Vahtrasa, M. A. Watson, D. J. D. Wilson, M. Ziolkowski, and H. Ågren. The dalton quantum chemistry program system, 2013.

[45] Avogadro: an open-source molecular builder and visualization tool. version 1.1. URL `http://avogadro.openmolecules.net/`.